Title

A Study to Investigate the Efficacy of Ethylenediamine Tetra-(Methylene Phosphonic Acid) as a Coating Material to Reduce the Toxicity of Upconversion Nanoparticles in Liver Cell Lines

Author

Hwang, Ruth Y

Publication Date

2019

Peer reviewed|Thesis/dissertation

UNIVERSITY OF CALIFORNIA

Los Angeles

A Study to Investigate the Efficacy of Ethylenediamine Tetra-(Methylene Phosphonic Acid) as a Coating Material to Reduce the Toxicity of Upconversion Nanoparticles in Liver Cell Lines

A thesis submitted in partial satisfaction

of the requirements for the degree Master of Science

in Environmental Health Sciences

by

Ruth Hwang

2019

ABSTRACT OF THE THESIS

A Study to Investigate the Efficacy of Ethylenediamine Tetra-(Methylene Phosphonic Acid) as a Coating Material to Reduce the Toxicity of Upconversion Nanoparticles in Liver Cell Lines

by

Ruth Hwang

Master of Science in Environmental Health Sciences
University of California, Los Angeles, 2019
Professor Yifang Zhu, Chair

Rare earth metals possess unique properties that make them extremely valuable for various industrial applications. Recently, there is a surge in the development of rare earth based upconversion nanoparticles (UCNPs) for biomedical applications including bioimaging and photothermal cancer therapy. Our findings on rare earth oxide nanoparticle biotransformation in an acidic environment and cytotoxicity raises safety concerns for rare earth based UCNPs. Although the health impacts of UCNPs have been carried out, they are mostly for lung effects after inhalation exposure and there are only limited studies on the effects of UCNPs on the liver. The liver is an important organ for nanotoxicological research because it is the primary bioaccumulation site for both incidental nanomaterials undergoing extrapulmonary translocation after inhalation and theranostic nanoparticles that are intravenously injected. This study aims to investigate the biotransformation pathways and mechanisms of toxicity of UCNPs to liver cells

and determine whether ethylenediamine tetra-(methylene phosphonic acid) (EDTMP) is a suitable protective coating material to prevent liver cell toxicity. Understanding this aspect is important for the development of safe UCNPs for biomedical applications. Liver cell viability was assessed after exposure to coated and non-coated UCNPs. The EDTMP coating material was effective in reducing the toxicity of certain UCNPs based on the dose and chemical composition, suggesting it could be a safer-by-design approach for UCNP biomedical applications.

The thesis of Ruth Hwang is approved.

Tian Xia

Shane S Que Hee

Michael D Collins

Yifang Zhu, Committee Chair

University of California, Los Angeles

2019

ACKNOWLEDGEMENTS

I would like to extend my gratitude to members of the Nanosafety Lab at the University of California Center for Environmental Implications of Nanotechnology: Drs. Tian Xia, Vahid Mirshafiee, Paul Chang, and Jinhong Jiang for mentoring and aiding me through each step of the laboratory experiment. Furthermore, I would like to thank Drs. Yifang Zhu, Hilary Godwin, Michael Collins, and Shane Que Hee for their commitment to students as faculty advisors and committee members in the Environmental Health Sciences Department. Additionally, I would like to thank Guarav Kandlikar, Caesar Li, and Adam Northrup for assisting me in writing and statistical techniques. Lastly, I am extremely grateful for the continual support of my friend Kailie Briza through this entire process.

TABLE OF CONTENTS

LIST OF FIGURES

1. INTRODUCTION

1.1 Objective and Rationale

Rare earth metals occur naturally in the environment and can also be engineered into nanoparticles for a variety of applications. Natural or anthropogenic exposures to rare earth nanomaterials can result in deleterious effects in plants, animals, and humans. Since the surge of applications utilizing rare earth nanomaterials, a series of studies have been conducted to understand their toxicity and how they can be made safer[1,2,3,4,5,6]. Indeed, rare earth oxide nanoparticles have been found to be toxic to mammalian cells and mouse lungs. Despite all this, there remains a knowledge gap on health impacts of a real-life application of rare earth-based nanomaterials, upconversion nanoparticles (UCNPs), which is a particle designed with various rare earth elements at certain percentages to enhance light absorption and emission. Based on previous literature on the toxicity of rare earth oxide nanoparticles, it is hypothesized that UCNPs could also induce cytotoxicity and ethylenediamine tetra(methylene phosphonic acid) (EDTMP) coating on UCNPs will reduce their toxicity in Kupffer (liver) cells. This project is a crucial step in understanding the toxic potential of rare earth nanomaterials with real-life relevance. The ultimate goal is to deepen the understanding of how different types of rare earth nanomaterials induce toxicity and the efficacy of a protective coating on UCNPs in liver cells. The study will characterize UCNPs with different compositions, examine their toxicity, and test the effectiveness of EDTMP coating in ameliorating the toxicity. The findings of this study will contribute to ongoing efforts in safer design of nanomaterials for medical applications including bioimaging, biosensing, and cancer treatment.

1.2 Importance, Application, and Toxicity of Nanomaterials

Nanoparticles, whether they are engineered for scientific and industrial purposes or formed as byproducts of industrial processes, are irrevocably found all around in society. Nanosized materials of all shapes and compositions possess novel properties that researchers can readily harness for technological advancement. A quick glance down a drugstore aisle will reveal items such as sunscreens, cosmetics, and powdered foods that contain nanoparticles[7,8]. For example, modern sunscreens contain titanium and zinc oxide nanoparticles that absorb and scatter UV lights, and their nano-size makes them transparent to avoid undesirable "white-out" effects[9,10]. Other common applications include, but are not limited to, products in transportation, electronics, agriculture, and medicine[7-8,11,12,13,14]. In medicine, physicians are continuously looking for new ways to improve diagnosis and treatments for patients. Engineered nanomaterials have the advantage of their small size to access previously inaccessible areas for targeted drug delivery and possess unique properties such as photoluminescence for bioimaging[3,15]. Furthermore, engineered nanomaterials can benefit the environment by enhancing current methods of waste water treatment by improving the photodegradation and reduction of dyes, organics, and pharmaceutical compounds[16,17]. Although engineered nanomaterials offer improvements not only to medicine but also many other industrial disciplines, these applications are dependent upon their safety profiles.

Among the various types of nanomaterials, rare earth materials are increasingly used in many industries for their magnetic, optical, and electronic properties[18]. In the process of extracting rare earth elements through rare earth mining and smelting, the generated aerosols present hazards not only to the workers but also to the public in surrounding areas. In the Bayan Obo mine in China, inhalation exposure to ultrafine rare earth containing dusts causes severe pulmonary diseases, which is an ongoing public health problem[19]. Increased demand among industries for rare

earth nanomaterials, leads to increased mining, separation, and consequently, increases possibilities of nanomaterial exposure to humans and the environment. Many studies have investigated engineered nanomaterials that are used in common consumer products such as silver and silica nanoparticles and have found that they can be toxic to humans, animals, plants, and aquatic species[20,21,22,23]. For each distinct type of nanomaterial, there are different physical and chemical properties that are responsible for their mechanism of toxicity. Some defining characteristics and factors that contribute to toxicity are size, shape, surface charge, aspect ratio, particle composition, and ion dissolution[24,25]. For example, analysis of zinc oxide nanoparticles indicates toxicity in mammalian cells and animals as a result of dissolution and the release of toxic zinc ions[2,5,26]. Similarly, silver nanoparticles are toxic and the mechanism involve dissolution and release of silver ions[27,28]. There are other mechanisms of toxicity induced by nanomaterials. For example, carbon nanotubes can rupture lysosomal membranes and result in inflammation and fibrosis due to high aspect ratios[29]. While the health hazards such as asthma, lung cancer, and cardiopulmonary disease from exposure to ambient ultrafine particles are well studied[30,31,32,33,34,35], less is understood on the magnitude that engineered nanoparticles contribute to diseases[36]. Thus, there is a need to study nanoparticles in a controlled setting to understand their mechanism of toxicity and pinpoint the properties that make them toxic. Focus should be given to industrially relevant nanomaterials since exposures to them are more likely to occur in real-life.

1.3 Rare Earth Oxide and Upconversion Nanoparticles

Recently, nanomaterials composed entirely or partially of rare earth oxide nanoparticles (REO NPs), are increasingly in use across numerous industries for their magnetic, optical, and electronic properties[18]. Among the seventeen rare earth elements, cerium (Ce), erbium (Er),

gadolinium (Gd), lanthanum (La), lutetium (Lu), neodymium (Nd), thulium (Tm), ytterbium (Yb), and yttrium (Y) are examples of commonly used REO NPs in industry for applications such as bio-imaging, catalysts, magnets, and batteries[18,37,38]. These materials possess unique luminescence properties that are particularly useful for improving medical imaging. For example, gadolinium is the base ingredient serving as magnetic resonance imaging (MRI) contrast agents[39]. While gadolinium can improve the image quality in MRI, there is a risk of nephrogenic systemic fibrosis in patients with renal impairment[40]. Furthermore, occupational exposures from mines to respirable ultrafine rare earth particles can cause coughing, inflammation, fibrosis, and eventually result in pneumoconiosis[41]. Other examples of commercial applications of rare earth nanomaterials are lanthanum for secondary batteries, exhaust and water purification, and yttrium for fluorescent lighting, fiber optics, and flat screen displays[42].

The unique properties of rare earth metals can be combined with other enhancing elements to create UCNPs. This real-life application involves the doping of a transition metal host lattice with two rare earth metal guest dopants. The guest dopants consist of an activator and sensitizer that work together to absorb and convert two or more low energy photons (near infrared light) into an emission of one high energy photon (ultra violet light)[6,38,43]. This nonlinear optical process of upconversion is known as anti-Stokes luminescence[44]. While still relatively new, UCNPs are being actively researched for medical applications including bioimaging, biosensing, and photothermal cancer therapy[45,46,47]. With increasing production and applications of rare earth nanomaterials, there is also a growing concern on the potential hazardous effects of these materials on the environment and humans.

1.4 Rare Earth Nanomaterial Toxicity

The unique properties that make rare earth nanomaterials useful may also render them toxic. In plants and animals, commercially available engineered nanoparticles such as cerium dioxide and lanthanum dioxide, are capable of entering, undergoing bio-transformation, and causing toxicity to plants and animals. The biotransformation process, whether it is in the soil surrounding plant roots or circulating to organs through an animals' body, plays an enormous role in the toxicity of rare earth nanomaterials[48,52]. For example, the rhizosphere that envelops roots with soil is rich in microbes, mucilage, organic acids, enzymes, and reducing substances, which form a microenvironment that can dissolve and reduce nanoparticles[48]. In a similar fashion, the acidic biological environment found in animal cells such as in lysosomes and macrophages, can dissolve rare earth nanomaterials, and the dissolved rare earth metal ions have a high binding affinity to phosphate groups. Rare earth ions binding with phosphates leads to the formation of needle-like or sea urchin-like structures. When phosphates in the lysosomal fluid are all consumed, the rare earth ions strip away phosphate groups from lysosomal membranes, causing lysosomal damage and releasing lysosomal enzymes including cathepsin B, which could activate NLRP3 inflammasomes leading to IL-1β production. IL-1β could trigger a series of events to epithelial cells and fibroblasts in the lung, leading to TGF-β and PDGF-AA secretion[25,49,50,51]. This chain of events can lead to pro-inflammatory effects, cell death, and fibrosis.

Although many studies have focused on REO NPs toxicity, toxicity of UCNPs is relatively less studied. It is reasonable to think that UCNPs could undergo similar biotransformation as REOs and could induce toxicity in a similar fashion. Indeed, a couple of studies observed that $NaYF_4$:Er/Yb, an UCNP, could undergo transformation in acidic biological media and be transformed into needle-like yttrium phosphate clusters[6,52]. These results are a clear indication that

UCNPs could also induce toxicity similar to that of REO NPs. In addition, this raises the question on how to inhibit UCNPs biotransformation and reduce toxicity.

1.5 Particle Coating as a Safer Design Method

Previously, it was demonstrated that a phosphate buffer solution could coat and reduce the toxic effects of rare earth oxide nanoparticles on THP-1 cells[49]. However, the protective effects of phosphate coating were only temporary. Therefore, phosphonates, which contain one or more C-$PO(OH)_2$ or C-PO-$(OR)_2$ groups were introduced with the hopes of increasing binding efficiency to rare earth atoms to prevent the dissolution of REOs, which is the critical first step of its biotransformation. Li *et al.* tested a variety of phosphate groups containing phosphonates including EDTMP, N-(phosphonomethyl)iminodiacetic acid, 3-(bromopropyl)phosphonic acid, and (aminomethyl)phosphonic acid as REO coating materials[6]. Among the four coating materials tested, EDTMP demonstrated the greatest particle stabilization in an acidic environment. Besides rare earth oxides, EDTMP is also an effective chelating agent for metal ions[53]. EDTMP has high affinity to metals such as copper, iron, zinc, nickel, cobalt, magnesium, and calcium[54]. This property makes EDTMP an ideal chemical to coat metal oxide nanoparticles that contain metals that are harmful to cells. Based on this data, it is hypothesized that EDTMP would also be effective in coating UCNPs and reduce their biotransformation and toxicity. Thus, the current study selected EDTMP to study its protective effects on UCNPs[6,49].

In addition to safety concerns, another important consideration on EDTMP coated nanoparticles is their function. In this case, it is the upconversion effects of UCNPs. If the particle is made safer but the UCNP loses its luminescent property and no longer can perform upconversion function, the purpose of coating is compromised[43]. A study found that 92% of cells treated with

EDTMP coated UCNPs still had fluorescence compared to only 18% fluorescent cells treated with pristine UCNPs after 24 hours. The implications of these results are that EDTMP coating on UCNPs does not compromise its photoluminescent property, but rather maintains photostability and imaging intensity. Although, the coating protects cells against the pro-inflammatory effects of THP-1 cells, the effects on REO induced Kupffer cell death is not clear[6].

Taking into consideration existing research, the challenge remains to determine whether EDTMP coating on UCNPs is an efficacious safer design method in liver cells, especially Kupffer cells, the first line of defense in the liver. To address this question, four relevant UCNPs with different chemical compositions and coatings including $NaYF_4$:Yb,Tm, $NaYF_4$:Yb,Er, $NaYF_4$:Yb,Er(polyethylene glycol (PEG) coated), and $NaYF_4$:Yb,Er(dense silica coated) were selected for the experiment. Previously, it was demonstrated in REO NPs that EDTMP is not completely protective of all types of nanoparticles, with some rare earth metals exhibiting higher toxicity than others. In order to increase the real-life relevance of our study, two types of UCNPs were selected with the goal to test different compositions of UCNPs in order to obtain a more complete picture. $NaYF_4$:Yb,Er and $NaYF_4$:Yb,Tm were selected based on their response to near-infrared irradiation by emitting multiple colors useful for various biolabeling and cancer treatment applications[55,56]. Additionally, polyethylene glycol (PEG) and dense silica (Silica) surface coatings were chosen on the erbium doped UCNP ($NaYF_4$:Yb,Er) to see the EDTMP coating effects in the presence of common surface coatings.

The particles were physically and chemically characterized to determine basic properties and coating efficiency. Following confirmation of EDTMP coating on the UCNPs, cell viability and imaging assays were completed to assess the effect of coated and non-coated particles in

Kupffer cells. Pristine particle toxicity and efficacy of EDTMP coating on reducing cell toxicity were subsequently analyzed, reported, and discussed in the following sections.

2. METHODS

2.1 Reagents and Materials

Two categories of nanomaterials were used in the experiments: REO NPs (Gd_2O_3, La_2O_3, Y_2O_3, and CeO_2) as control nanoparticles based on our previous published reports and UCNPs ($NaYF_4$:Yb,Tm, $NaYF_4$:Yb,Er, $NaYF_4$:Yb,Er(PEG coated), and $NaYF_4$:Yb,Er(dense silica coated)). Gd_2O_3 and La_2O_3 were purchased from Nanostructured and Amorphous Materials, Inc. (Katy, TX) while Y_2O_3 and CeO_2 were purchased from Meliorum Technologies (Rochester, NY). The four upconversion nanoparticles were purchased from Creative Diagnostics (Shirley, NY). Ethylenediamine tetra-(methylene phosphonic acid) (EDTMP) with 95% purity, the particle coating material, was purchased from Santa Cruz Biotechnologies (Santa Ana, CA) (Table S1. Supplementary Information).

KUP5, an immortalized Kupffer cell line established from the C57BL/6 mouse strain and transformed by the human *c-myc* oncogene, was purchased from RIKEN CELL BANK (Ibaraki, Japan). Reagents obtained for KUP5 cells include DMEM cell culture media (Thermo Fisher Scientific, Waltham, MA), bovine insulin (Sigma - Aldrich, St. Louis, MO), trypsin (Thermo Fisher Scientific, Waltham, MA), 1-thioglycerol (Sigma - Aldrich, St. Louis, MO), Lipopolysaccharides (LPS) (Sigma - Aldrich, St. Louis, MO), and 10% fetal bovine serum and antibiotics prepared in-house.

Assay kits used in the experiment include the CellTiter 96® Aqueous 5-(3-carboxymethoxyphenyl)-2-(4,5-dimenthylthiazoly)-3-(4-sulfophenyl)tetrazolium (MTS) Assay

Reagent (Promega, Madison, WI), CytoTox 96® Non-Radioactive Cytotoxicity Assay (Promega, Madison, WI), and Magic Red Cathepsin B Assay Kit (ImmunoChemistry Technologies LLC, Bloomington, MN).

2.2 Cell Culture

A KUP5 cell stock was passaged and grown in DMEM cell culture media that was further supplemented with 50 mL of 10% fetal bovine serum, 10 μg/mL of bovine insulin (500 μL), and 250 μM of 1-Thioglycerol (11 μL). Cells were incubated in sterile conditions at 37° C with 5% CO_2 and passaged at approximately 80% confluency.

2.3 Surface Coating

The following EDTMP coating procedure was adopted from Li *et al*.[6]. A solution of 20 mL of deionized H_2O containing 8 mg (400 μg/mL) of EDTMP was prepared in a 50 ml falcon tube. 4 mg (200 μg/mL) of each nanoparticle was separately dispersed in the EDTMP solution and stirred with a magnetic stir bar on a magnetic stirrer at room temperature for 24 hours, resulting in a 2:1 coating to particle ratio. Following the 24-hour incubation period, the solution containing the nanoparticles was washed with 2 mL of deionized H_2O three times by centrifugation at 5000 rpm, removal of the supernatant, and resuspension of the pellet with deionized H_2O. Finally, after the last wash, the EDTMP-coated nanoparticles were resuspended in deionized H_2O and stored at 4° C. As previously mentioned, increased coating and incubation period were tested to determine the most efficacious coating parameters.

2.4 Physical Characterization of Nanoparticles

Pristine, coated, and phagolysosomal simulated fluid (PSF) transformed nanoparticles were characterized by transmission electron microscopy (TEM) on a JEOL 1200 EX instrument (accelerating voltage 80 kV). Particles for TEM analysis were prepared in deionized H_2O at concentration 50 μg/mL. The samples were fixed with 2.5% glutaraldehyde solution, embedded in resin, cut into ultrathin sections by an ultramicrotome with a diamond knife, and collected on a copper grid. A final stain with uranyl acetate and lead citrate was applied before imaging at 500,000X magnification.

Fourier transform infrared (FTIR) spectra were collected with Bruker Vertex 70 instrument. A minimum of 1 mg of dried nanoparticle was required and prepared for analysis by drying H_2O suspended nanoparticles in a scientific medium laboratory oven. The FTIR instrument applied IR of 10,000 cm^{-1} through each sample. While some of the radiation was scattered, the absorbed radiation was converted into vibrational energy which was detected by the instrument and read as a spectrum (4000 to 400 cm^{-1}).

2.5 Assessment of EDTMP Coating Effectiveness

In order to conduct a preliminary assessment of EDTMP coating success, the coated nanoparticles were challenged in a PSF buffer. The PSF buffer was formulated with 142 mg/L Na_2HPO_4, 6,650 mg/L NaCl, 62 mg/L Na_2SO_4, 29 mg/L $CaCl_4$-H_2O, 250 mg/L glycine, and 8,090 mg/L $C_8H_5KO_4$, in 1 L of deionized H_2O at pH 4.5[49]. Coated particles were added to 10 mL of PSF buffer at 50 μg/mL in 15 mL falcon tubes and incubated at 37° C for 24 hours. Following incubation, the mixture was centrifuged at 10,000 rpm for 10 minutes and washed with 2 mL of deionized H_2O three times. Lastly, the particles were resuspended in 100 μl of deionized H_2O. The integrity and condition of the particles before and after the PSF buffer challenge were visualized

and assessed with images obtained by TEM (Figure S1a. Supplementary Information). Additional coating ratios (5:1 and 10:1) and incubation period (48 hours) were tested to determine the most efficacious coating parameters (Table S2 and Figure S1b. Supplementary Information).

2.6 Determination of Cellular Viability

KUP5 cell viability to UCNPs was assessed with the MTS assay (CellTiter 96® Aqueous MTS Assay Reagent). Cells were incubated for 24 hours at 37° C to seat them into 96-well microtiter plates (Corning® Costar® TC-Treated 96-Well Plates) at a density of 2 x 10^4 cells per well. Following incubation, the cells were treated with LPS at 1 μg/mL for 4 hours. Immediately after the incubation time, the LPS was removed with a pipet and nanoparticles were added at concentrations 0, 6.25, 12.5, 25, 50, 100, and 200 μg/mL with three replicates. The cells were incubated with the nanoparticles for 24 hours at 37° C. MTS reagent was diluted with cell culture media at a 1:5 reagent to media ratio. The post-nanoparticle exposure supernatant was removed with a multi-channel pipet (stored at -80° C for later use in a 96-well plate) before the MTS reagent solution was added and incubated with the cells for 1 hour at 37° C. Lastly, the 96-well plate was centrifuged and the supernatant transferred to another 96-well plate with a multi-channel pipet to read the absorbance at 490 nm in a Biotek absorbance reader.

2.7 Assessment of Cytotoxicity

In order to determine UCNP cytotoxicity, cell death was assessed with the Lactate Dehydrogenase (LDH) release assay (CytoTox 96® Non-Radioactive Cytotoxicity Assay). KUP5 cells were seated at 2 x 10^4 cells per well and primed with 1 μg/mL LPS for 4 hours. The positive control was prepared with a lysis solution from the assay kit for maximum LDH release. After exposing the cells to LPS for 4 hours, LPS was removed and the cells were exposed to 200 ug/mL

of each nanoparticle for 24 hours. The supernatant was collected into a 96-well plate and incubated at room temperature with the CytoTox 96® Reagent for 30 minutes. The plate was wrapped in foil to protect the contents from light. After a stop solution was added, the absorbance was read at 490 nm on a Biotek absorbance reader.

2.8 Confocal Microscopy Imaging of Lysosomal Integrity

Using the Magic Red Cathepsin B Assay Kit, KUP5 cells were seated overnight at 37° C in 8-well Lab-Tek chamber slides at a density of 5 x 10^4 cells. The cells were primed with LPS (1 µg/mL) for 4 hours and exposed to nanoparticles (50 µg/mL) for 1 hour. Uniformity of coverage was of nanoparticles was confirmed under a microscope. Following exposure, the cells were incubated with 2 µL of Magic Red Cathepsin B working solution for 30 minutes at 37° C. The Magic Red Cathepsin B substrate is supplied as a lyophilized powder which is reconstituted with 200 µl of DMSO. This reconstituted stock is diluted 1:10 with deionized H_2O then added to cells at a 1:26 ratio. The cells were then fixed with 4% paraformaldehyde in phosphate buffer solution (PBS) in order to preserve cell morphology. Lastly, the cells were stained with 2 µL of Hoechst 33342 (5 µg/mL) and imaged at 100,000X magnification under a Leica Confocal SP8-SMD microscope with excitation filter of 365 nm and emission of 480 nm. Three areas from each treatment were randomly selected and imaged. Images were analyzed with Image J software to obtain corrected total cell fluorescence (CTCF). CTCF was corrected for background noise in the images.

2.9 Statistical Analysis

Using historical data, sample sizes were calculated to achieve an effect level of at least 1-5% difference in cell viability. A minimum of 3 samples per treatment group is admissible in order

to draw statistical conclusions with a Student's t-Test at 90% power and 0.05 alpha level. The following formula was used for sample size calculations:

$$n_i = \frac{\left(Z_{1-\frac{\alpha}{2}} + Z_{1-\beta}\right)^2}{\Delta^2}\text{s}$$

Where $\Delta = \frac{\mu_2 - \mu_1}{\sigma^2}$

In sample calculations specified above, σ^2 is estimated by pooled variance, and it's given by:

$$S_{pooled} = \frac{(n_1 - 1)S_1^2 + (n_2 - 1)S_2^2}{n_1 + n_2 - 2}$$

MTS data was collected in the form of absorbance values. The negative control values were averaged to obtain a healthy cell baseline absorbance value. Each individual negative control value was then divided by the baseline mean and multiplied by 100 and averaged together to achieve a cell viability percentage for the negative control. The absorbance values from the experimental samples were analyzed in the same way to obtain a mean percentage of cell viability for each particle type and dose. For each particle type, the dose at which the greatest difference between the two treatment groups (EDTMP-coated and non-coated) was calculated by finding the difference in means. A two-sample Student t-Test assuming unequal variances was then used to determine whether the differences in means were significant. The same approach was taken for LDH absorbance and confocal microscopy fluorescence data.

3. RESULTS

3.1 REO NP Coating and Abiotic transformation in PSF

While the focus of this project is UCNPs, the coating method was first tested on control REO NPs to determine the best coating ratio and incubation time. Based on Li *et al.*'s coating

method, a 2:1 EDTMP to nanoparticle weight ratio and 24-hour incubation period was chosen[6]. Additionally, a PBS coating, a 5:1 and a 10:1 EDTMP coating ratio, and a 48-hour incubation period were tested. PBS was not an effective protective coating (data not shown), nor were increased coating ratios and incubation time of EDTMP (Figure S1b. Supplementary Information). Thus, for the most efficacious coating strategy, it was decided to use a 2:1 coating ratio and 24-hour incubation period.

Furthermore, in order to determine the robustness and quality of EDTMP coating on REO NPs, a PSF challenge was completed. PSF (pH 4.5) is a cell free simulated acidic media present in lysosomes in cells. The REO NPs were assessed by TEM images comparing before and after exposure to PSF. The results demonstrate that EDTMP is effective at preventing abiotic transformation of La_2O_3 and CeO_2 nanoparticle but less protective of Gd_2O_3 and Y_2O_3 nanoparticles (Figure S1a. Supplementary Information). This is an indication of expected differential levels of toxicity between different rare earth nanomaterials. Therefore, EDTMP is more effective at preventing abiotic transformation of REO NPs in acidic biological media for certain REOs than others. From these data, the coating experiment was continued with commercially available UCNPs.

3.2 UCNP Physical Chemical Characterization

The four UCNPs were obtained from a commercial source which came with basic particle information such as diameter, storage buffer, and size distribution. Each particle was further characterized in-house to obtain a thorough profile in order to better understand their properties, which are useful in building a toxicity relationship for the UCNPs.

TEM is a technique used to visualize and characterize nanomaterial structures in media, plants, and animal tissues. A beam of electrons is transmitted through a prepared sample to form an image. The UCNPs were prepared at 50 µg/mL in H_2O and imaged with and without EDTMP coating. The images showed the same morphology between pristine and EDTMP coated UCNPs (Figure 1a). This is an expected result as a coating should not alter the shape and size of nanoparticles. Consistent with the commercially provided information, primary particle diameters ranged from 20 to 40 nm. $NaYF_4$:Yb,Tm however formed some particle agglomerates with sizes greater than 50 nm. The shapes of the particles are predominantly circular or hexagonal.

The TEM images revealed no differences between the pristine and EDTMP-coated UCNPs. Therefore, in order to confirm that the particles had been successfully coated with EDTMP, FTIR spectra was collected and analyzed. The absorbance peaks seen in Figure 2 are labelled accordingly to indicate functional groups present in each type of nanoparticle. A solid red line represents EDTMP-coated UCNPs and a dotted black line represents the non-coated UCNP. In figures 2b and 2d, there is a distinguishable peak labelled P=O at approximately 1000 cm^{-1} wavenumber for EDTMP-coated particles. This peak is characteristic of the P=O group found in EDTMP and is not present in the absorbance profiles of the non-coated particles. Figures 2a and 2c however, do not display distinct P=O peaks.

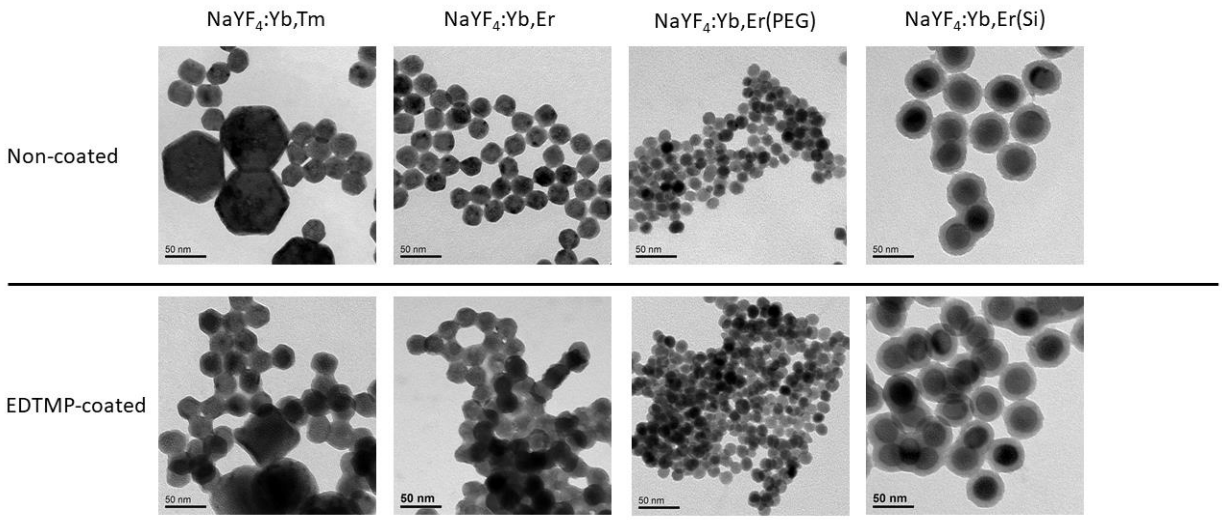

Figure 1. Physical characterization of UCNPs by TEM show no change in morphology between the non-coated and EDTMP-coated UCNPs.

a) $NaYF_4$:Yb,Er(PEG)

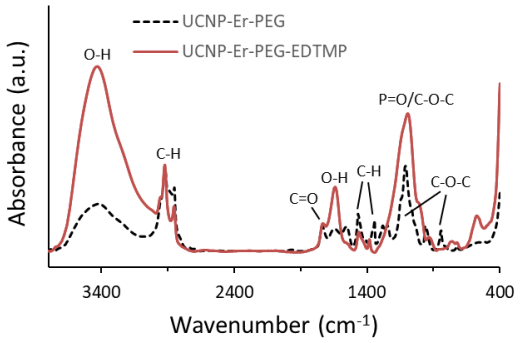

b) $NaYF_4$:Yb,Er

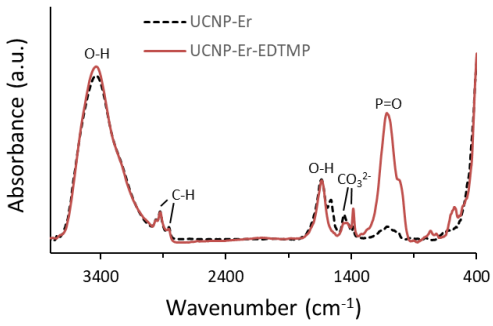

c) $NaYF_4$:Yb,Er(silica)

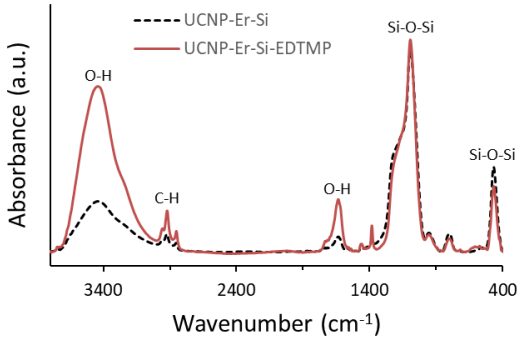

d) $NaYF_4$:Yb,Tm

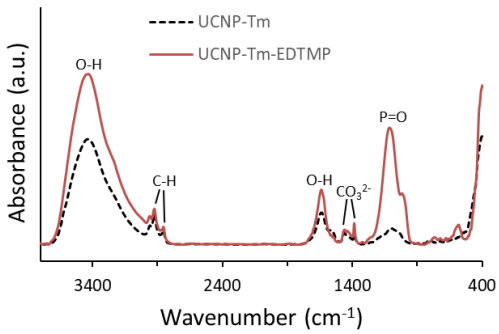

Figure 2. Chemical characterization of UCNPs by FTIR demonstrates presence of EDTMP coating. Graphs **b)** and **d)** show a distinct P=O peak in the EDTMP-coated particles that is not present in the non-coated particles. This indicates the successful coating of EDTMP onto the UCNPs. Graphs **a)** and **c)** however do not have distinct P=O peaks. This is likely due to the existing PEG and dense silica coating on the $NaYF_4$:Yb,Er particles. **a)** $NaYF_4$:Yb,Er(PEG). **b)** $NaYF_4$:Yb,Er. **c)** $NaYF_4$:Yb,Er(silica). **d)** $NaYF_4$:Yb,Tm.

3.3 Determination of UCNP toxicity in KUP5 Cells

KUP5 cells were exposed to a range of UCNPs ranging from a concentration of 0-200 μg/mL (0, 6.25, 12.5, 25, 50, 100, 200 μg/mL). This dose range was decided and based upon other studies on metal oxide toxicity in the liver[1,25,57,58]. The toxicological analysis was first completed with the MTS cellular viability assay. MTS, is a tetrazolium salt compound that is biologically reduced by living cells into a formazan product[59]. This conversion relies on NADPH or NADH produced by dehydrogenase enzymes in cells. The presence of dehydrogenase enzymes is a measure of a cell's viability. Therefore, the absorbance intensity of formazan is proportional to the number of metabolically active living cells in culture. The dose-response curves for three of the four UCNPs clearly indicate a significant difference in cell viability when exposed to particles for 24 hours with and without EDTMP coating (Figure 3). Without EDTMP coating for all four UCNPs, at concentrations of 50 μg/mL and lower, cell viability stays above 50% for all UCNPs. Greater than 50 μg/mL decreases viability to approximately 20-30%. Of the four particles, EDTMP-coated $NaYF_4$:Yb,Er(PEG) (Figure 3a) displayed the greatest significant cell viability difference to the non-coated $NaYF_4$:Yb,Er(PEG). Between the coated and non-coated groups, the greatest difference was 47% ($p < 0.05$) at 100 μg/mL. $NaYF_4$:Yb,Er similarly showed percent viability improvement but to a lesser extent with a 23% difference at 6.25 μg/mL ($p < 0.05$). KUP5 exposed EDTMP-coated $NaYF_4$:Yb,Er(silica) exhibited improved viability only at doses equal to

or lower than 50 µg/mL. There is the greatest difference of 17% at 6.25 µg/mL ($p < 0.05$). Cells exposed to the thulium doped particle, $NaYF_4$:Yb,Tm, did not display any improvement in viability. The greatest difference in means was only 0.37% at 12.5 µg/mL ($p > 0.05$). Overall for the UCNPs with a significant difference in means between the coated and non-coated treatments, there was an approximate 20-50% viability improvement.

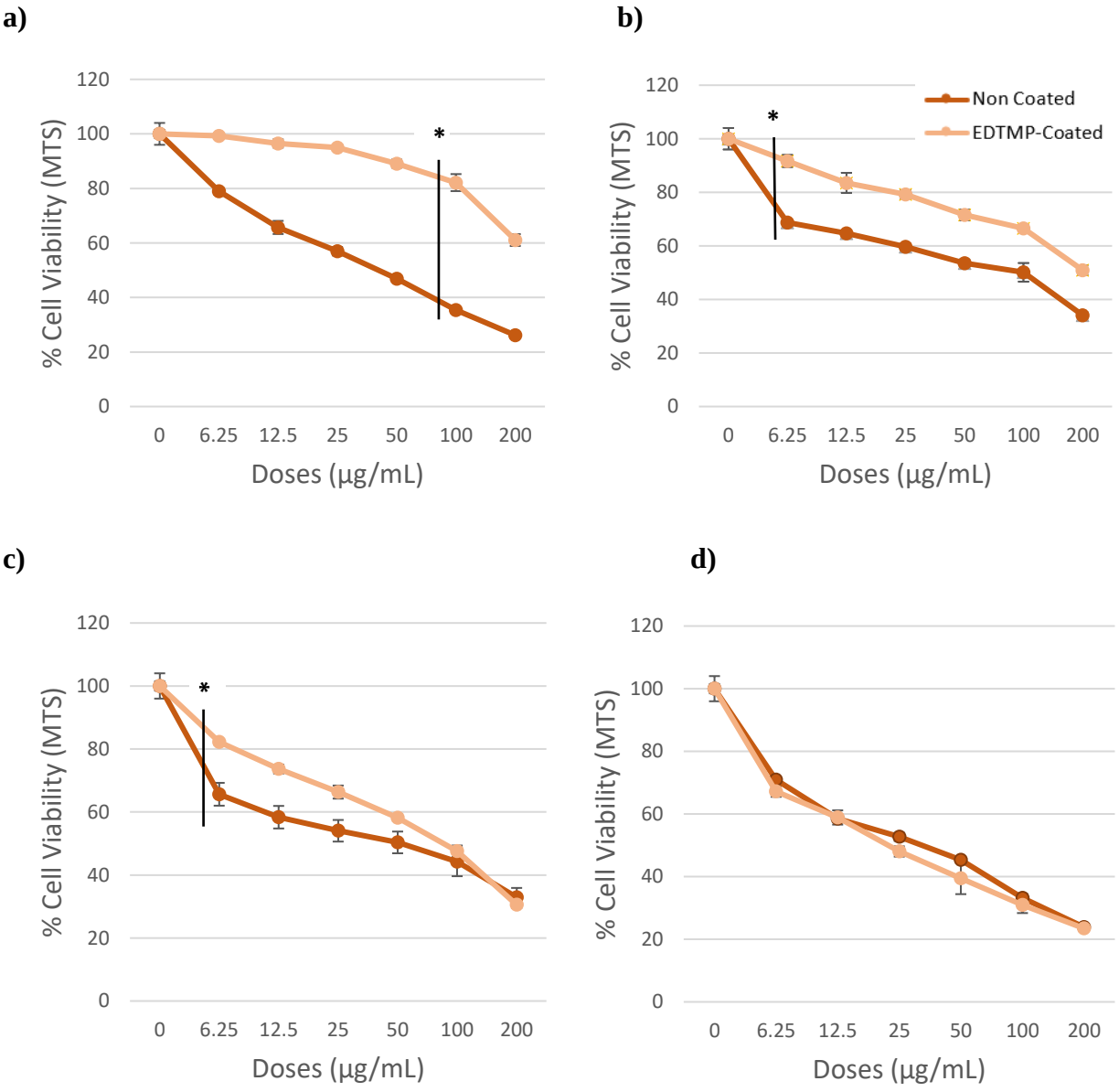

Figure 3. Graphs a) through d) demonstrate in order from least to most toxic, the differences in KUP5 cellular viability (MTS assay) when exposed to non-coated and EDTMP-coated UCNPs. **a)** $NaYF_4$:Yb,Er(PEG). **b)** $NaYF_4$:Yb,Er. **c)** $NaYF_4$:Yb,Er(silica). **d)** $NaYF_4$:Yb,Tm. *$p < 0.05$.

To further investigate toxicity to UCNPs, KUP5 cytotoxicity was determined with the LDH assay. While the MTS assay quantifies living cells, the LDH assay quantifies dead lysed cells. Lactate dehydrogenase (LDH) is an enzyme found in the cytoplasm of cells. When there is a loss of membrane integrity due to various stressors including exposure to xenobiotics, LDH is released. This is a phenomenon characteristic of membrane damage and cell death. The assay is capable of measuring LDH release from cell membrane damage by quantifying the conversion of a tetrazolium salt (iodonitro-tetrazolium violet; INT) by LDH into a formazan product[60,61]. The highest dose of 200 μg/mL UCNPs from the MTS assay was used to measure cell death as the endpoint. The results from the LDH assay (Figure 4) closely parallel those from the MTS assay. EDTMP coating on $NaYF_4$:Yb,Tm had no effect on reducing cytotoxicity. The other three particles exhibited significant differences with p-values < 0.05 in toxicity between the non-coated and EDTMP coated groups, consistent with the cell viability results by MTS assay (Figure 3). From the non-coated to EDTMP-coated $NaYF_4$:Yb,Er, $NaYF_4$:Yb,Er(silica), and $NaYF_4$:Yb,Er(PEG) there was an approximate 42%, 39%, and 37% decrease in cytotoxicity, respectively.

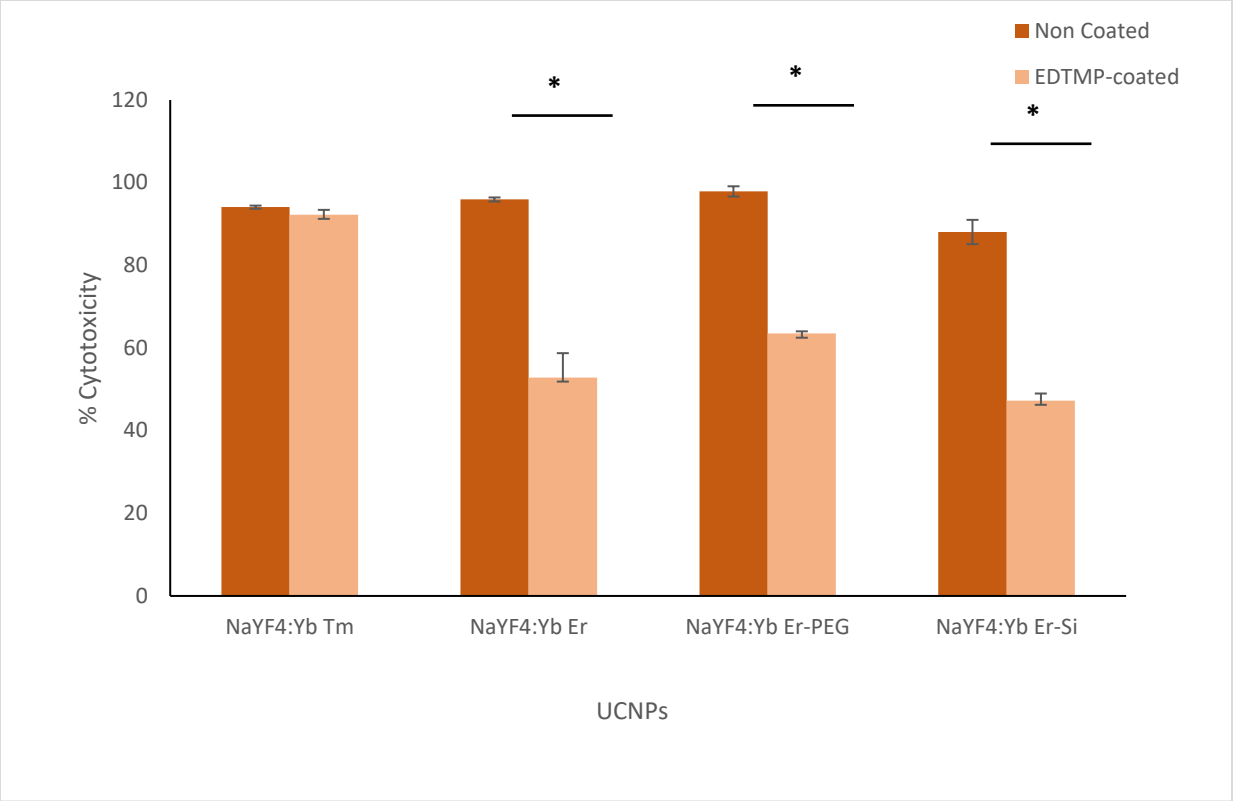

Figure 4. Cell death measured by LDH release from KUP5 cells exposed to non-coated and EDTMP-coated UCNPs. * $p < 0.05$.

3.4 Evaluation of Lysosomal Intactness

It is known that cells take up UCNPs which accumulate in lysosomes, potentially leading to lysosomal damage. To study lysosomal damage, KUP5 cells exposed to UCNPs, were fixed and stained with Hoechst 33342 and Magic Red Substrate. Three sections of each treatment, with and without EDTMP coating, were randomly selected to be imaged. One of three images for each treatment was randomly selected and displayed in Figure 5. Nuclei are labeled in blue with Hoechst 33342 to help locate each individual cell. Magic red substrate fluoresces red when cleaved by cathepsin B, a lysosomal cysteine protease. Therefore, red in the images shows damaged lysosomes. A higher intensity of red fluorescence indicates greater damage to cells and therefore

cell viability. The confocal images show that EDTMP coating on UCNPs is slightly protective in KUP5 cells. With the exception of $NaYF_4$:Yb,Tm, the non-coated treatments display greater counts of red fluorescence per cell. Image J analysis was performed to quantify the total cell fluorescence. A cell was randomly selected from each image and measured for area, integrated density, and mean fluorescence of background readings. Integrated density is the sum of the values of the pixels in the image. A corrected total cell fluorescence (CTCF) was calculated and averaged for each UCNPs by multiplying the area of a selected cell by the mean fluorescence of background readings and subtracting it from the integrated density. The CTCFs of EDTMP-coated and non-coated UCNPs are displayed in Figure 5b. Although EDTMP coating reduced the fluorescence intensity for all UCNPs, significant difference in mean CTCFs between the two treatments was found only for $NaYF_4$:Yb,Er(PEG).

(a)

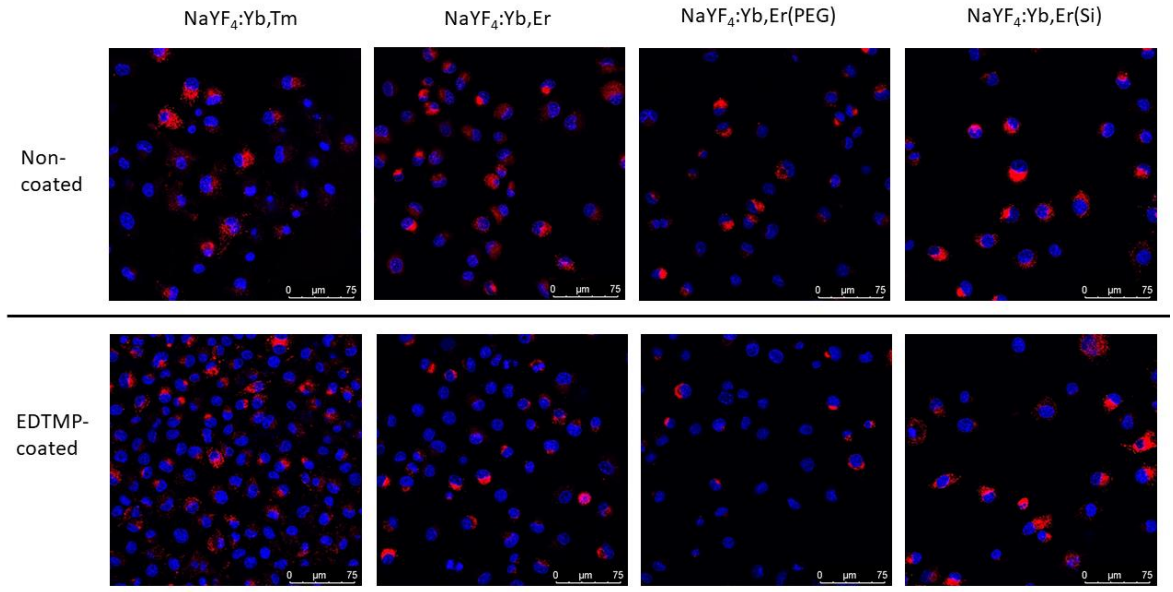

b)

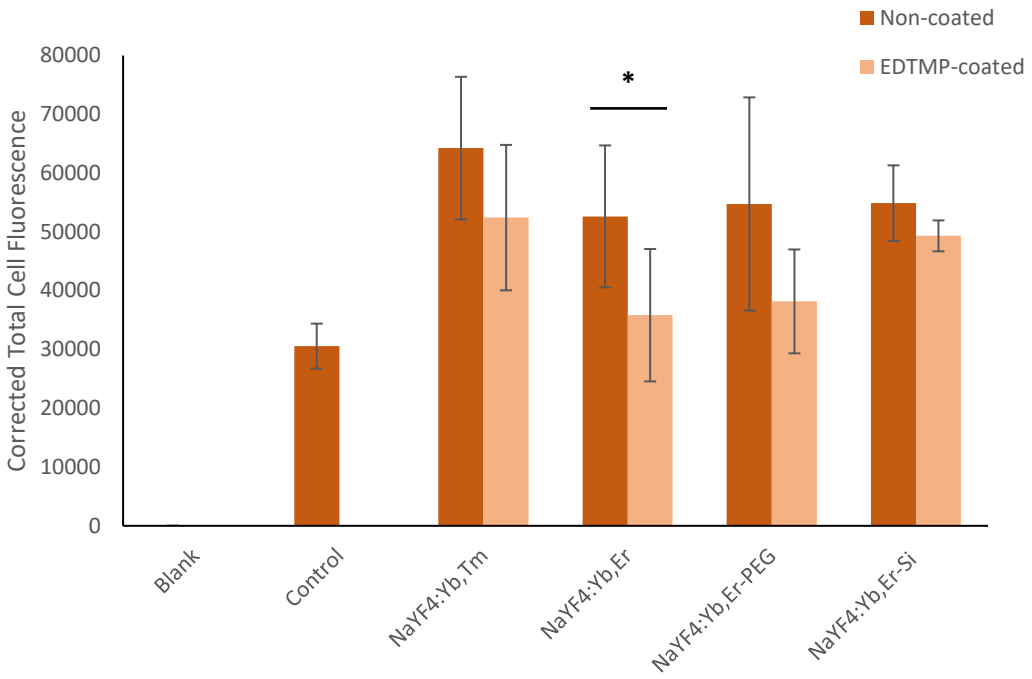

Figure 5. Confocal microscopy images of KUP5 cells and corresponding corrected total cell fluorescence derived from Image J Analysis. **a)** Nuclei are labelled in blue and lysosomal enzymes in red. **b)** Corrected total cell fluorescence with higher fluorescence values indicate a greater extent of damage to KUP5 cell lysosomes. *p < 0.05.

4. DISCUSSION

4.1 Summary of Results

In this study, four commercially available UCNPs were characterized and assessed in KUP5 liver cells to understand their properties and cytotoxicity relationships. Each particle was coated with EDTMP and compared to their pristine counterparts. The most important finding in this study is that an EDTMP coating can significantly reduce the toxicity of certain UCNPs. Additionally, the results indicate that certain UCNPs are more toxic than others due to their dopants and coatings. KUP5 cells were on average more viable when exposed to EDTMP-coated erbium than thulium UCNPs. Within erbium-doped UCNPs, PEG and silica coating contributed to

differential toxicities as well. Despite the variable protective effects of EDTMP coating, overall it is a potentially promising safer design material.

4.2 EDTMP Coating onto UCNPs is Confirmed with TEM and FTIR

TEM images provide a physical assessment of a coating on a material while FTIR gives a definitive confirmation on the presence of a coating. FTIR analysis is therefore essential to confirming the presence and successful coating of the EDTMP coating onto UCNPs. TEM images in Figure 1 indicated no morphological differences between coated and non-coated particles. Unsurprisingly, EDTMP coating did not alter the physical but rather the chemical properties of a nanoparticle. In the images for $NaYF_4$:Yb,Er(silica), the dense silica coating is clearly visible as a lighter grey ring around a darker circle. However, coatings such as PEG and EDTMP, are not electron dense and thus are not visible by TEM. FTIR graphs on the other hand provide a chemical snapshot of a material and therefore presence of coatings could be confirmed. The distinct P=O peak for $NaYF_4$:Yb,Er and $NaYF_4$:Yb,Tm confirmed the presence of the phosphonate coating onto the particles. For the other two UCNPs, $NaYF_4$:Yb,Er(PEG) had a slight P=O peak, while $NaYF_4$:Yb(Silica) had no distinguishable P=O peak. Since $NaYF_4$:Yb,Er is able to be successfully coated with EDTMP, theoretically, $NaYF_4$:Yb,Er(PEG) and $NaYF_4$:Yb,Er(silica) should be as well. However, it is possible that the existing coatings (PEG and silica) on $NaYF_4$:Yb,Er interfered with the proper coating of EDTMP and therefore were not clearly identified by FTIR. Although the coating is not well confirmed for these two particles as seen in Figures 2a and 2c, the difference between the two treatments observed in the following assays is sufficient evidence to conclude that the particles are coated with EDTMP.

4.3 Chemical Composition and Dose affects Particle Toxicity and Cell Viability

A dose-response curve is fundamental to understanding a xenobiotics hazardous potential and toxicity. In vitro analysis of KUP5 cell viability after exposure to different concentrations of EDTMP coated and non-coated UCNPs revealed the differential toxicities of the two metal dopants, Er and Tm, and surface coatings, PEG and silica. MTS data showed that all four pristine UCNPs, had similar baseline toxicities in terms of cellular viability. Starting at 100% viability for untreated KUP5 cells, viability gradually decreased to approximately 30% with increased UCNP concentrations. However, when coated with EDTMP, $NaYF_4$:Yb,Er-PEG exposed KUP5 cells demonstrated the greatest increase in cell viability, whereas $NaYF_4$:Yb,Tm exposed KUP5 were not protected by the EDTMP coating (Figure 2(a)). KUP5 exposed to EDTMP-$NaYF_4$:Yb,Er and EDTMP-$NaYF_4$:Yb,Er-silica had increased viability but to a lesser degree than EDTMP-$NaYF_4$:Yb,Er-PEG. The difference between UCNPs doped with thulium versus those doped with erbium was more noticeable. Thulium (Tm) and erbium (Er) are the rare earth metal dopants (activators) that set the nanoparticles chemically apart. Under the current test conditions, the results of the MTS cell viability assay indicate the inherent cytotoxicity of each different particle. The order of particle toxicities is clearly demonstrated from least toxic in Figure 2(a) to most toxic in Figure 2(d). With EDTMP-coating, cell viability improves from 25% to 60% when the concentration of $NaYF_4$:Yb,Er-PEG is at the highest dose (200 μg/mL), even after 24 hours of incubation. From these results, it can be concluded that EDTMP coating is most effective in reducing $NaYF_4$:Yb,Er-PEG UCNP induced- cytotoxicity compared to the other three UCNPs.

To confirm these differences in toxicities, cystolic LDH released from KUP5 cells, an indicator of cell membrane integrity, was additionally measured. LDH levels detected in this assay is equivalent to the proportion of lysed cells. Overall, the LDH assay results reflect those of the

MTS cell viability assay (Figure 3). There is however a dramatic decrease in % cytotoxicity for EDTMP-coated $NaYF_4$:Yb,Er-(silica) at 200 μg/mL whereas the cell viability does not increase at the same dose. These results reflect the sensitivity of the LDH assay in low-level cytotoxicity detection and may indicate that among the viable cells, there is a proportion that have disrupted or damaged membranes but are not detected as viable in the MTS assay. Therefore, EDTMP can be partially protective on $NaYF_4$:Yb,Er-(silica) at higher concentrations.

The results of the MTS and LDH assays raise the question of why there are differential toxicities between the dopants and coating materials. PEG is a polar hydrophilic polymer that has been demonstrated to be a biologically inert coating material that reduces nanoparticle cytotoxicity and increases water solubility for biological applications[4,56,62]. Similarly, a silica coating makes nanoparticles more dispersible in water and has good *in vitro* and *in vivo* biocompatibility[58,63]. However, studies have shown that amorphous silica nanoparticles can induce oxidative stress, inflammation, and apoptosis in KUP5 cells[25,64]. While both coating materials are useful to increase dispersibility and biocompatibility of UCNPs in biomedical applications, their inherent properties are a possible explanation to the differential toxicities of EDTMP-coated $NaYF_4$:Yb,Er-PEG and $NaYF_4$:Yb,Er-silica. Meanwhile, there are numerous studies on the bioimaging capabilities of $NaYF_4$:Yb,Tm, however, little to no studies on its toxicity in the liver. In fact, there is research that indicates $NaYF_4$:Yb,Tm has low toxicity and is safe[65,66]. Such studies use different cell lines from different species and cytotoxicity assays; therefore, it is difficult to compare the results of this study to others. As rare earth materials gain momentum in industry, there still remains a knowledge gap on their toxicokinetics and toxicodynamics. Research to thoroughly map out and understand metabolism and mechanisms of toxicity for different UCNPs should be prioritized. Completing

the picture of a novel material's properties and toxicity profiles will establish a baseline that allows for future research advancement.

The confocal microscopy images of KUP5 cells provide a qualitative visual aid to assess lysosomal health. The lysosome is a key organelle for processing and digesting endocytosed foreign bodies such as nanoparticles. Thus, if lysosomes are compromised, a cell's ability to protect itself from potentially toxic xenobiotics is also compromised. The negative control image shows punctate red fluorescence, indicating healthy viable cells (Figure 4(a) control panel). The few red spots visible are as expected since even in non-exposed populations, not all cells will be healthy. KUP5 cells exposed to both EDTMP-coated and non-coated UCNPs displayed high levels of red fluorescence, indicating lysosomal damage and cathepsin B release. Despite the slight protective effect of an EDTMP coating, cell viability is still compromised to an extent as indicated by damaged lysosomes. While there is some discrepancy in cell density seen particularly between the coated and non-coated $NaYF_4$:Yb,Tm images, overall, there does not appear to be a decrease in cells with damaged lysosomes, but rather an increase. For $NaYF_4$:Yb,Er, $NaYF_4$:Yb,Er-PEG, and $NaYF_4$:Yb,Er-silica, there is a slight decrease in cells with compromised lysosomes. Quantifiable CTCF converted from the confocal microscopy images by Image J analysis allows for the measurement of lysosomal damage. Despite the overall trend that suggests KUP5 exposed EDTMP-coated UCNPs experience less lyososomal rupturing, there is a high level of variability in the data. The variability potentially arises from human error in light adjustments and image area selection during imaging. Although differences were found between the EDTMP-coated and non-coated treated cell viabilities, a significant difference was found only for $NaYF_4$:Yb,Er. Despite of challenges to obtain consistent confocal images and quantify the data, lysosomal intactness presents itself as an important indicator of cell death and toxicity of an UCNPs.

4.4 Limitations and Next Steps

While there are numerous ways to evaluate cellular viability, the MTS, LDH, and Magic Red Cathepsin B assays were selected based on the merits of cost, feasibility of completion in a relatively short time period, and availability of experimental equipment. Without financial and temporal constraints, it would have been ideal to use a much larger library of UCNPs and a greater variety of assays to measure cell viability and other factors such as inflammatory cytokines. The current work is preliminary in nature and there remains numerous aspects of UCNP toxicity that need to be explored and studied. Next steps include the introduction of animal studies to better understand EDTMP coated UCNP *in vivo* toxicity and interaction with metal nutrients in the body. Additionally, there is a need to test more biocompatible coating materials since the results of this study demonstrated that EDTMP is not protective of all nanoparticles. Another benefit of continued exploration of physicochemical properties and cytotoxicity of different UCNPs, is to discover novel materials that may substitute the toxic materials with less toxic ones. A better understanding of mechanisms of toxicity provides a baseline to develop safer design methods while still maintaining application of the material.

5. CONCLUSIONS

The three cytotoxicity endpoints, cell viability, LDH leakage, and lysosomal integrity, were assessed in this study, which represent indicators of biological function to provide a preliminary understanding of a material's toxicity. EDTMP is a biocompatible coating material that not only does not alter the upconversion function of the particle but also reduces its cytotoxicity on three of the four UCNPs investigated. EDTMP coating on $NaYF_4$:Yb,Er, $NaYF_4$:Yb,Er-PEG, and $NaYF_4$:Yb,Er-silica were more effective than $NaYF_4$:Yb,Tm. There was a significant difference

in percent cellular viability of 47%, 23%, and 17% and decrease in cytotoxicity of 37%, 42%, and 39% of Kupffer cells exposed to non-coated and EDTMP-coated $NaYF_4$:Yb,Er-PEG, $NaYF_4$:Yb,Er, and $NaYF_4$:Yb,Er-silica, respectively. The findings of this study contribute to the overall understanding of rare earth nanomaterial toxicity and provide insights to their mechanisms of toxicity and subsequent health risk and impact assessments. Furthermore, an understanding of how different coating materials affect a particles' toxicity can help researchers to make decisions on suitable materials for safer biomedical applications.

6. SUPPLEMENTARY INFORMATION

Nanoparticle	Manufacturer	Diameter (nm)
Gd_2O_3	Nanostructured Amorphous Materials, Inc.	15 - 30
La_2O_3	Nanostructured Amorphous Materials, Inc.	15 - 30
Y_2O_3	Meliorum Technologies	8 - 10
CeO_2	Meliorum Technologies	8 - 10
$NaYF_4$:Yb,Tm	Creative Diagnostics	30
$NaYF_4$:Yb,Er	Creative Diagnostics	30
$NaYF_4$:Yb,Er(PEG coated)	Creative Diagnostics	30
$NaYF_4$:Yb,Er(dense silica coated)	Creative Diagnostics	30

Table S1. List of nanoparticles and their respective manufacturers and size in diameters.

Nanoparticle	**2:1**	**5:1**	**10:1**	**24 Hours**	**48 Hours**	**Effect**
Gd_2O_3	✓	✓	✓	✓		Increased coating ratio is not protective
La_2O_3	✓			✓		Coating highly protective
Y_2O_3	✓	✓	✓	✓	✓	Increased coating ratio is not protective
CeO_2	✓			✓		CeO_2 is non - toxic / no change
$NaYF_4$:Yb,Tm	✓			✓		Coating not protective

$NaYF_4$:Yb,Er	✓			✓		Coating moderately protective
$NaYF_4$:Yb,Er(PEG coated)	✓			✓		Coating highly protective
$NaYF_4$:Yb,Er(dense silica coated)	✓			✓		Coating protective

Table S2. The effects of different EDTMP coating ratios and incubation periods. Higher coating ratios were not protective and particles did not maintain their morphology.

a)

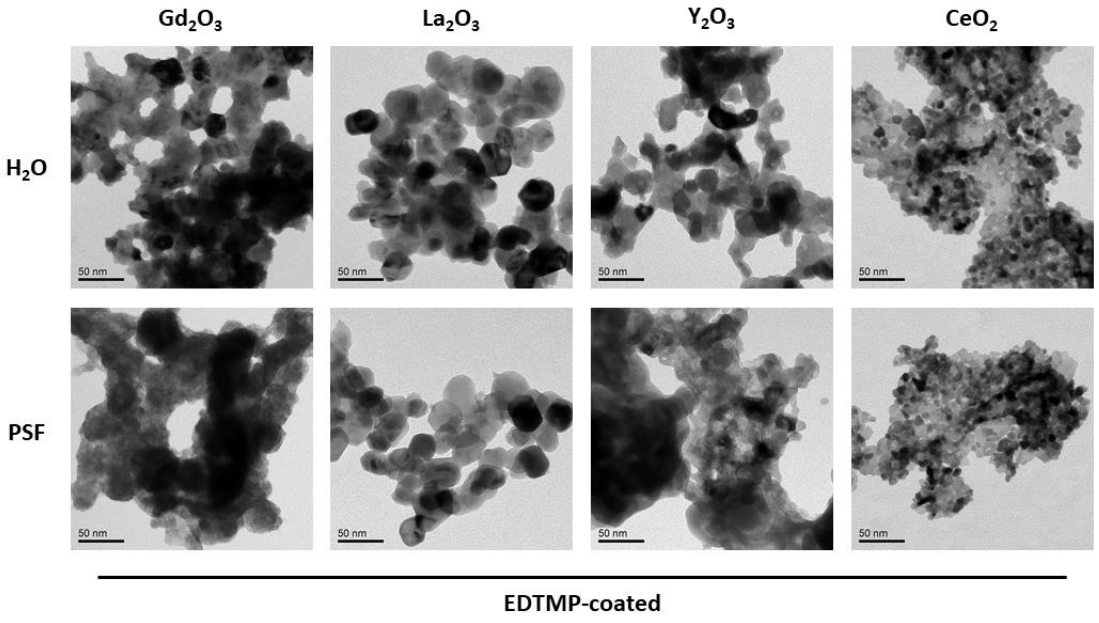

b)

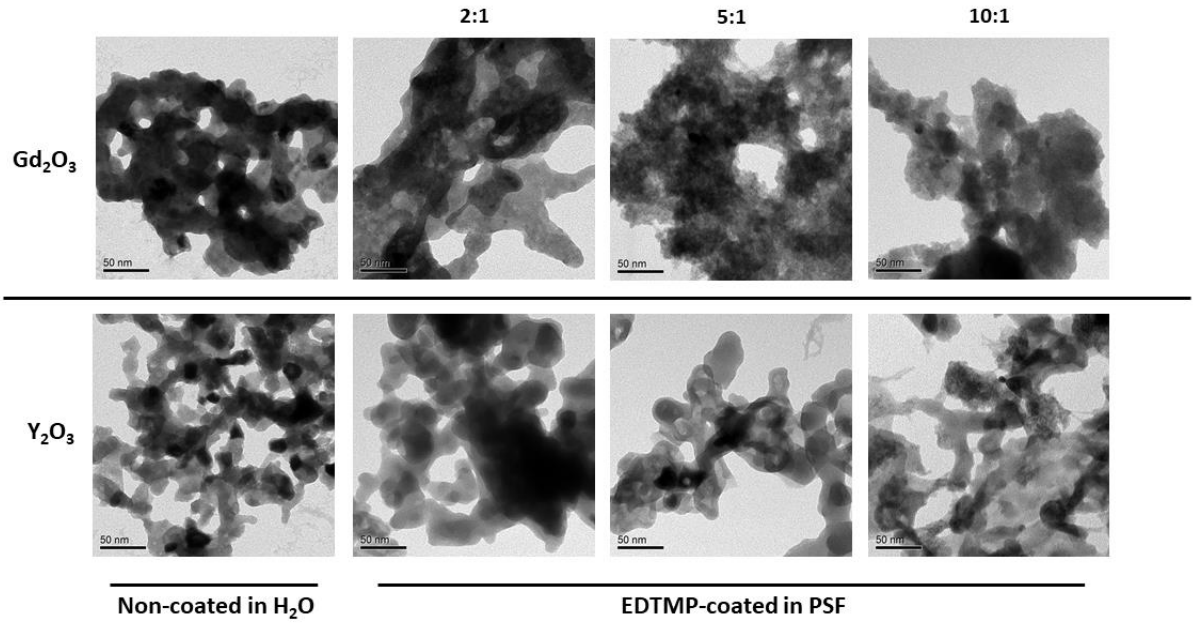

Figure S1. TEM images of non-coated and EDTMP coated REO NPs in PSF and H_2O with different coating ratios and incubation periods. (a) EDTMP coated Gd_2O_3, La_2O_3, Y_2O_3, and CeO_2 were exposed to PSF to determine effectiveness of the 2:1 coating. (b) Following the PSF challenge with all the REO NPs, Gd_2O_3 and Y_2O_3, were selected for further testing since the 2:1 EDTMP coating was not protective. Additional coating ratios 5:1 and 10:1 were tested along with an increased incubation period of 24 hours. Scale bars are 50 nm.

7. REFERENCES

1. Hussain, S. M.; Hess, K. L.; Gearhart, J. M.; Geiss, K. T.; Schlager, J. J., In vitro toxicity of nanoparticles in BRL 3A rat liver cells. *Toxicology in Vitro* **2005,** *19* (7), 975-983.

2. Xia, T.; Kovochich, M.; Liong, M.; Mädler, L.; Gilbert, B.; Shi, H.; Yeh, J. I.; Zink, J. I.; Nel, A. E., Comparison of the Mechanism of Toxicity of Zinc Oxide and Cerium Oxide Nanoparticles Based on Dissolution and Oxidative Stress Properties. *ACS Nano* **2008,** *2* (10), 2121-2134.

3. Yildirimer, L.; Thanh, N. T. K.; Loizidou, M.; Seifalian, A. M., Toxicology and clinical potential of nanoparticles. *Nano Today* **2011,** *6* (6), 585-607.

4. Gnach, A.; Lipinski, T.; Bednarkiewicz, A.; Rybka, J.; Capobianco, J. A., Upconverting nanoparticles: assessing the toxicity. *Chemical Society Reviews* **2015,** *44* (6), 1561-1584.

5. George, S.; Pokhrel, S.; Xia, T.; Gilbert, B.; Ji, Z.; Schowalter, M.; Rosenauer, A.; Damoiseaux, R.; Bradley, K. A.; Mädler, L.; Nel, A. E., Use of a Rapid Cytotoxicity Screening Approach To Engineer a Safer Zinc Oxide Nanoparticle through Iron Doping. *ACS Nano* **2010,** *4* (1), 15-29.

6. Li, R.; Ji, Z.; Dong, J.; Chang, C. H.; Wang, X.; Sun, B.; Wang, M.; Liao, Y.-P.; Zink, J. I.; Nel, A. E.; Xia, T., Enhancing the Imaging and Biosafety of Upconversion Nanoparticles through Phosphonate Coating. *ACS Nano* **2015,** *9* (3), 3293-3306.

7. Stark, W. J.; Stoessel, P. R.; Wohlleben, W.; Hafner, A., Industrial applications of nanoparticles. *Chem Soc Rev* **2015,** *44* (16), 5793-805.

8. Vance, M. E.; Kuiken, T.; Vejerano, E. P.; McGinnis, S. P.; Hochella, M. F., Jr.; Rejeski, D.; Hull, M. S., Nanotechnology in the real world: Redeveloping the nanomaterial consumer products inventory. *Beilstein J Nanotechnol* **2015,** *6*, 1769-80.

9. Lu, P.-J.; Huang, S.-C.; Chen, Y.-P.; Chiueh, L.-C.; Shih, D. Y.-C., Analysis of titanium dioxide and zinc oxide nanoparticles in cosmetics. *Journal of Food and Drug Analysis* **2015,** *23* (3), 587-594.

10. Lorenz, C.; Tiede, K.; Tear, S.; Boxall, A.; Von Goetz, N.; Hungerbühler, K., Imaging and Characterization of Engineered Nanoparticles in Sunscreens by Electron Microscopy, Under Wet and Dry Conditions. *International Journal of Occupational and Environmental Health* **2010,** *16* (4), 406-428.

11. Ji, Z.; Wang, X.; Zhang, H.; Lin, S.; Meng, H.; Sun, B.; George, S.; Xia, T.; Nel, A. E.; Zink, J. I., Designed synthesis of CeO2 nanorods and nanowires for studying toxicological effects of high aspect ratio nanomaterials. *ACS Nano* **2012,** *6* (6), 5366-80.

12. Contreras, J. E.; Rodriguez, E. A.; Taha-Tijerina, J., Nanotechnology applications for electrical transformers—A review. *Electric Power Systems Research* **2017,** *143*, 573-584.

13. Martinkova, P.; Brtnicky, M.; Kynicky, J.; Pohanka, M., Iron Oxide Nanoparticles: Innovative Tool in Cancer Diagnosis and Therapy. *Advanced Healthcare Materials* **2018,** *7* (5), 1700932.

14. Muthu, M. S.; Leong, D. T.; Mei, L.; Feng, S.-S., Nanotheranostics - application and further development of nanomedicine strategies for advanced theranostics. *Theranostics* **2014,** *4* (6), 660-677.

15. Zhang, L.; Gu, F.; Chan, J.; Wang, A.; Langer, R.; Farokhzad, O., Nanoparticles in Medicine: Therapeutic Applications and Developments. *Clinical Pharmacology & Therapeutics* **2008,** *83* (5), 761-769.

16. Devi, T. B.; Ahmaruzzaman, M., Bio-inspired facile and green fabrication of Au@Ag@AgCl core–double shells nanoparticles and their potential applications for elimination of toxic emerging pollutants: A green and efficient approach for wastewater treatment. *Chemical Engineering Journal* **2017,** *317*, 726-741.

17. Hou, C.; Jiao, T.; Xing, R.; Chen, Y.; Zhou, J.; Zhang, L., Preparation of TiO2 nanoparticles modified electrospun nanocomposite membranes toward efficient dye degradation for wastewater treatment. *Journal of the Taiwan Institute of Chemical Engineers* **2017,** *78*, 118-126.

18. Bouzigues, C.; Gacoin, T.; Alexandrou, A., Biological Applications of Rare-Earth Based Nanoparticles. *ACS Nano* **2011,** *5* (11), 8488-8505.

19. Wang, L.; Zhong, B.; Liang, T.; Xing, B.; Zhu, Y., Atmospheric thorium pollution and inhalation exposure in the largest rare earth mining and smelting area in China. *Science of The Total Environment* **2016,** *572*, 1-8.

20. Jiang, W.; Lin, S.; Chang, C. H.; Ji, Z.; Sun, B.; Wang, X.; Li, R.; Pon, N.; Xia, T.; Nel, A. E., Implications of the Differential Toxicological Effects of III–V Ionic and Particulate Materials for Hazard Assessment of Semiconductor Slurries. *ACS Nano* **2015,** *9* (12), 12011-12025.

21. Osborne, O. J.; Lin, S.; Chang, C. H.; Ji, Z.; Yu, X.; Wang, X.; Lin, S.; Xia, T.; Nel, A. E., Organ-Specific and Size-Dependent Ag Nanoparticle Toxicity in Gills and Intestines of Adult Zebrafish. *ACS Nano* **2015,** *9* (10), 9573-9584.

22. Nel, A.; Xia, T.; Mädler, L.; Li, N., Toxic Potential of Materials at the Nanolevel. *Science* **2006,** *311* (5761), 622.

23. Dekkers, S.; Krystek, P.; Peters, R. J. B.; Lankveld, D. P. K.; Bokkers, B. G. H.; van Hoeven-Arentzen, P. H.; Bouwmeester, H.; Oomen, A. G., Presence and risks of nanosilica in food products. *Nanotoxicology* **2011,** *5* (3), 393-405.

24. Hwang, R.; Mirshafiee, V.; Zhu, Y.; Xia, T., Current approaches for safer design of engineered nanomaterials. *Ecotoxicology and Environmental Safety* **2018,** *166*, 294-300.

25. Mirshafiee, V.; Sun, B.; Chang, C. H.; Liao, Y.-P.; Jiang, W.; Jiang, J.; Liu, X.; Wang, X.; Xia, T.; Nel, A. E., Toxicological Profiling of Metal Oxide Nanoparticles in Liver Context Reveals Pyroptosis in Kupffer Cells and Macrophages versus Apoptosis in Hepatocytes. *ACS Nano* **2018,** *12* (4), 3836-3852.

26. Liu, J.; Feng, X.; Wei, L.; Chen, L.; Song, B.; Shao, L., The toxicology of ion-shedding zinc oxide nanoparticles. *Critical Reviews in Toxicology* **2016,** *46* (4), 348-384.

27. Hou, J.; Zhou, Y.; Wang, C.; Li, S.; Wang, X., Toxic Effects and Molecular Mechanism of Different Types of Silver Nanoparticles to the Aquatic Crustacean Daphnia magna. *Environmental Science & Technology* **2017,** *51* (21), 12868-12878.

28. Wang, X.; Ji, Z.; Chang, C. H.; Zhang, H.; Wang, M.; Liao, Y.-P.; Lin, S.; Meng, H.; Li, R.; Sun, B.; Winkle, L. V.; Pinkerton, K. E.; Zink, J. I.; Xia, T.; Nel, A. E., Use of Coated Silver Nanoparticles to Understand the Relationship of Particle Dissolution and Bioavailability to Cell and Lung Toxicological Potential. *Small* **2014,** *10* (2), 385-398.

29. Wang, X.; Xia, T.; Duch, M. C.; Ji, Z.; Zhang, H.; Li, R.; Sun, B.; Lin, S.; Meng, H.; Liao, Y.-P.; Wang, M.; Song, T.-B.; Yang, Y.; Hersam, M. C.; Nel, A. E., Pluronic F108 Coating Decreases the Lung Fibrosis Potential of Multiwall Carbon Nanotubes by Reducing Lysosomal Injury. *Nano Letters* **2012,** *12* (6), 3050-3061.

30. Liu, S.; Xia, T.; Zhu, Y.; Mu, L.; Zhang, Z.-F., Pulmonary diseases induced by ambient ultrafine and engineered nanoparticles in twenty-first century. *National Science Review* **2016,** *3* (4), 416-429.

31. Oberdörster, G., Pulmonary effects of inhaled ultrafine particles. *International Archives of Occupational and Environmental Health* **2000,** *74* (1), 1-8.

32. Donaldson, K.; Brown, D.; Clouter, A.; Duffin, R.; MacNee, W.; Renwick, L.; Tran, L.; Stone, V., The Pulmonary Toxicology of Ultrafine Particles. *Journal of Aerosol Medicine* **2002,** *15* (2), 213-220.

33. Morawska, L.; Ristovski, Z.; Jayaratne, E. R.; Keogh, D. U.; Ling, X., Ambient nano and ultrafine particles from motor vehicle emissions: Characteristics, ambient processing and implications on human exposure. *Atmospheric Environment* **2008,** *42* (35), 8113-8138.

34. Gilmour, P. S.; Ziesenis, A.; Morrison, E. R.; Vickers, M. A.; Drost, E. M.; Ford, I.; Karg, E.; Mossa, C.; Schroeppel, A.; Ferron, G. A.; Heyder, J.; Greaves, M.; MacNee,

W.; Donaldson, K., Pulmonary and systemic effects of short-term inhalation exposure to ultrafine carbon black particles. *Toxicology and Applied Pharmacology* **2004,** *195* (1), 35-44.

35. Frampton, M. W.; Utell, M. J.; Zareba, W.; Oberdörster, G.; Cox, C.; Huang, L.-S.; Morrow, P. E.; Lee, F. E.-H.; Chalupa, D.; Frasier, L. M.; Speers, D. M.; Stewart, J., Effects of exposure to ultrafine carbon particles in healthy subjects and subjects with asthma. *Res Rep Health Eff Inst* **2004,** (126), 1-47; discussion 49-63.

36. Oberdörster, G.; Oberdörster, E.; Oberdörster, J., Nanotoxicology: An Emerging Discipline Evolving from Studies of Ultrafine Particles. *Environmental Health Perspectives* **2005,** *113* (7), 823-839.

37. Xu, C.; Qu, X., Cerium oxide nanoparticle: a remarkably versatile rare earth nanomaterial for biological applications. *Npg Asia Materials* **2014,** *6*, e90.

38. Gai, S.; Li, C.; Yang, P.; Lin, J., Recent Progress in Rare Earth Micro/Nanocrystals: Soft Chemical Synthesis, Luminescent Properties, and Biomedical Applications. *Chemical Reviews* **2014,** *114* (4), 2343-2389.

39. Thomsen, H. S.; Morcos, S. K.; Almén, T.; Bellin, M.-F.; Bertolotto, M.; Bongartz, G.; Clement, O.; Leander, P.; Heinz-Peer, G.; Reimer, P.; Stacul, F.; van der Molen, A.; Webb, J. A., Nephrogenic systemic fibrosis and gadolinium-based contrast media: updated ESUR Contrast Medium Safety Committee guidelines. *European Radiology* **2013,** *23* (2), 307-318.

40. Marckmann, P.; Skov, L.; Rossen, K.; Dupont, A.; Damholt, M. B.; Heaf, J. G.; Thomsen, H. S., Nephrogenic Systemic Fibrosis: Suspected Causative Role of Gadodiamide Used for Contrast-Enhanced Magnetic Resonance Imaging. *Journal of the American Society of Nephrology* **2006,** *17* (9), 2359.

41. Vocaturo, G.; Colombo, F.; Zanoni, M.; Rodi, F.; Sabbioni, E.; Pietra, R., Human Exposure to Heavy Metals: Rare Earth Pneumoconiosis in Occupational Workers. *Chest* **1983,** *83* (5), 780-783.

42. Rim, K. T.; Koo, K. H.; Park, J. S., Toxicological Evaluations of Rare Earths and Their Health Impacts to Workers: A Literature Review. *Safety and Health at Work* **2013,** *4* (1), 12-26.

43. Wang, F.; Banerjee, D.; Liu, Y.; Chen, X.; Liu, X., Upconversion nanoparticles in biological labeling, imaging, and therapy. *Analyst* **2010,** *135* (8), 1839-1854.

44. Chatterjee, D. K.; Gnanasammandhan, M. K.; Zhang, Y., Small Upconverting Fluorescent Nanoparticles for Biomedical Applications. *Small* **2010,** *6* (24), 2781-2795.

45. Cheng, L.; Yang, K.; Li, Y.; Chen, J.; Wang, C.; Shao, M.; Lee, S.-T.; Liu, Z., Facile Preparation of Multifunctional Upconversion Nanoprobes for Multimodal Imaging and Dual-Targeted Photothermal Therapy. *Angewandte Chemie* **2011,** *123* (32), 7523-7528.

46. Kobayashi, H.; Longmire, M. R.; Ogawa, M.; Choyke, P. L., Rational chemical design of the next generation of molecular imaging probes based on physics and biology: mixing modalities, colors and signals. *Chemical Society Reviews* **2011,** *40* (9), 4626-4648.

47. Kumar, R.; Nyk, M.; Ohulchanskyy, T. Y.; Flask, C. A.; Prasad, P. N., Combined Optical and MR Bioimaging Using Rare Earth Ion Doped NaYF4 Nanocrystals. *Advanced Functional Materials* **2009,** *19* (6), 853-859.

48. Zhang, P.; Ma, Y.; Zhang, Z.; He, X.; Zhang, J.; Guo, Z.; Tai, R.; Zhao, Y.; Chai, Z., Biotransformation of Ceria Nanoparticles in Cucumber Plants. *ACS Nano* **2012,** *6* (11), 9943-9950.

49. Li, R.; Ji, Z.; Chang, C. H.; Dunphy, D. R.; Cai, X.; Meng, H.; Zhang, H.; Sun, B.; Wang, X.; Dong, J.; Lin, S.; Wang, M.; Liao, Y.-P.; Brinker, C. J.; Nel, A.; Xia, T., Surface Interactions with Compartmentalized Cellular Phosphates Explain Rare Earth Oxide Nanoparticle Hazard and Provide Opportunities for Safer Design. *ACS Nano* **2014,** *8* (2), 1771-1783.

50. Lin, S.; Wang, X.; Ji, Z.; Chang, C. H.; Dong, Y.; Meng, H.; Liao, Y.-P.; Wang, M.; Song, T.-B.; Kohan, S.; Xia, T.; Zink, J. I.; Lin, S.; Nel, A. E., Aspect Ratio Plays a Role in the Hazard Potential of CeO2 Nanoparticles in Mouse Lung and Zebrafish Gastrointestinal Tract. *ACS Nano* **2014,** *8* (5), 4450-4464.

51. Sisler, J. D.; Li, R.; McKinney, W.; Mercer, R. R.; Ji, Z.; Xia, T.; Wang, X.; Shaffer, J.; Orandle, M.; Mihalchik, A. L.; Battelli, L.; Chen, B. T.; Wolfarth, M.; Andrew, M. E.; Schwegler-Berry, D.; Porter, D. W.; Castranova, V.; Nel, A.; Qian, Y., Differential pulmonary effects of CoO and La2O3 metal oxide nanoparticle responses during aerosolized inhalation in mice. *Particle and Fibre Toxicology* **2016,** *13* (1), 42.

52. Yin, W.; Zhou, L.; Ma, Y.; Tian, G.; Zhao, J.; Yan, L.; Zheng, X.; Zhang, P.; Yu, J.; Gu, Z.; Zhao, Y., Phytotoxicity, Translocation, and Biotransformation of NaYF4 Upconversion Nanoparticles in a Soybean Plant. *Small* **2015,** *11* (36), 4774-4784.

53. Westerback, S. J.; Martell, A. E., Ethylene-diamine-tetra(methylene-phosphonic) Acid. *Nature* **1956,** *178* (4528), 321-322.

54. Motekaitis, R. J.; Murase, I.; Martell, A. E., Equilibriums of ethylenediamine-N, N, N', N'-tetrakis (methylenephosphonic) acid with copper (II), nickel (II), cobalt (II), zinc (II), magnesium (II), calcium (II), and iron (III) ions in aqueous solution. *Inorganic Chemistry* **1976,** *15* (9), 2303-2306.

55. Wang, M.; Mi, C.; Zhang, Y.; Liu, J.; Li, F.; Mao, C.; Xu, S., NIR-Responsive Silica-Coated NaYbF4:Er/Tm/Ho Upconversion Fluorescent Nanoparticles with Tunable Emission Colors and Their Applications in Immunolabeling and Fluorescent Imaging of Cancer Cells. *The Journal of Physical Chemistry C* **2009,** *113* (44), 19021-19027.

56. Chen, X.; Zhao, Z.; Jiang, M.; Que, D.; Shi, S.; Zheng, N., Preparation and photodynamic therapy application of NaYF4:Yb, Tm–NaYF4:Yb, Er multifunctional upconverting nanoparticles. *New Journal of Chemistry* **2013,** *37* (6), 1782-1788.

57. Kermanizadeh, A.; Gaiser, B. K.; Hutchison, G. R.; Stone, V., An in vitro liver model - assessing oxidative stress and genotoxicity following exposure of hepatocytes to a panel of engineered nanomaterials. *Particle and Fibre Toxicology* **2012,** *9* (1), 28.

58. Abdul Jalil, R.; Zhang, Y., Biocompatibility of silica coated NaYF4 upconversion fluorescent nanocrystals. *Biomaterials* **2008,** *29* (30), 4122-4128.

59. Barltrop, J. A.; Owen, T. C.; Cory, A. H.; Cory, J. G., 5-(3-carboxymethoxyphenyl)-2-(4,5-dimethylthiazolyl)-3-(4-sulfophenyl)tetrazolium, inner salt (MTS) and related analogs of 3-(4,5-dimethylthiazolyl)-2,5-diphenyltetrazolium bromide (MTT) reducing to purple water-soluble formazans As cell-viability indicators. *Bioorganic & Medicinal Chemistry Letters* **1991,** *1* (11), 611-614.

60. Korzeniewski, C.; Callewaert, D. M., An enzyme-release assay for natural cytotoxicity. *Journal of Immunological Methods* **1983,** *64* (3), 313-320.

61. Lappalainen, K.; Jääskeläinen, I.; Syrjänen, K.; Urtti, A.; Syrjänen, S., Comparison of Cell Proliferation and Toxicity Assays Using Two Cationic Liposomes. *Pharmaceutical Research* **1994,** *11* (8), 1127-1131.

62. Yu, M.; Huang, S.; Yu, K. J.; Clyne, A. M., Dextran and Polymer Polyethylene Glycol (PEG) Coating Reduce Both 5 and 30 nm Iron Oxide Nanoparticle Cytotoxicity in 2D and 3D Cell Culture. *International Journal of Molecular Sciences* **2012,** *13* (5), 5554.

63. Li, Z.; Zhang, Y., Monodisperse Silica-Coated Polyvinylpyrrolidone/NaYF4 Nanocrystals with Multicolor Upconversion Fluorescence Emission. *Angewandte Chemie* **2006,** *118* (46), 7896-7899.

64. Kojima, S.; Negishi, Y.; Tsukimoto, M.; Takenouchi, T.; Kitani, H.; Takeda, K., Purinergic signaling via P2X7 receptor mediates IL-1β production in Kupffer cells exposed to silica nanoparticle. *Toxicology* **2014,** *321*, 13-20.

65. Zhou, J.-C.; Yang, Z.-L.; Dong, W.; Tang, R.-J.; Sun, L.-D.; Yan, C.-H., Bioimaging and toxicity assessments of near-infrared upconversion luminescent NaYF4:Yb,Tm nanocrystals. *Biomaterials* **2011,** *32* (34), 9059-9067.

66. Peng, J.; Sun, Y.; Liu, Q.; Yang, Y.; Zhou, J.; Feng, W.; Zhang, X.; Li, F., Upconversion nanoparticles dramatically promote plant growth without toxicity. *Nano Research* **2012,** *5* (11), 770-782.